



Research article

Integration of ion transport membrane with conventional powerplant to enhance the plant capacity with improved power production

Arnob Das^{a,*}, Susmita Datta Peu^b, Md Sanowar Hossain^a, Barun Kumar Das^a

^a Department of Mechanical Engineering, Rajshahi University of Engineering and Technology, Rajshahi, 6204, Bangladesh

^b Department of Agriculture, Hajee Mohammad Danesh Science and Technology University, Dinajpur, 5200, Bangladesh

ARTICLE INFO

Keywords:

IGCC
Ion transport membrane
Air separator
Gas turbine
Gasifier
HRSG

ABSTRACT

Ion Transport Membrane (ITM) is an emerging technology for producing O₂ by separating air in its membrane. To decrease energy loss in air separation unit and to increase the overall efficiency of a power generation unit ITM is added with the gasification unit in this model. Ceramic materials are generally used to make the ion transport membrane that produces oxygen by conducting oxygen ions at a specified temperature. Potential advantages can be gained by integrating ITM technology with power generation units as 99% pure oxygen is produced from ITM. Using ITM air separator is more beneficial compared to cryogenic air separation as ITM technology helps to improve IGCC overall efficiency and also reduces plant auxiliaries than that of power generation systems integrated with cryogenic. This paper proposed a novel and effective integration of ITM, gas turbine, HRSG system, gas clean up system and gasification unit to produce sustainable energy. Environmental impacts are considered to design this integrated power generation unit. The proposed model achieved a high gross electric efficiency of 47.58% and high net power of 296730 kW which revealed its potentiality compared to available cryogenic ASU-based combine cycle power plants.

1. Introduction

The energy demand has been increased with increased population and growth of different power sectors [1,2]. From the past decades the development of Integrated Gasification Combined Cycle (IGCC) has started and in recent years it is widely used as power generation system. IGCC system has some potential advantages like low amount of sulfur, less NO_x, higher thermal efficiency, and higher CO₂ capturing capacity in pre-combustion stage [3–6]; however, it requires more development and optimization for global utilization [7]. A high plant efficiency ranging from 28 to 40% can be achieved via IGCC technology [8–10] as well as generate other valuable chemicals such as methanol, hydrogen which can reduce the dependency on fossil fuels [11,12].

Model of an oxygen-blown IGCC using an Ion Transport Membrane (ITM) to produce oxygen, instead of a conventional cryogenic system, is proposed in this study. Currently, the most common way to produce oxygen is by pressure swing absorption, and cryogenic air separation [13]. These processes are well-proven, but energy intensive, lower O₂ purity, and expensive to build and operate [14,

* Corresponding author. Department of Mechanical Engineering, Rajshahi University of Engineering & Technology, Rajshahi, 6204, Bangladesh.
E-mail addresses: arnobarjun@gmail.com (A. Das), susmitapeu77@gmail.com (S.D. Peu), sanowar122086@gmail.com (M.S. Hossain), bkdas@me.ruet.ac.bd (B.K. Das).

<https://doi.org/10.1016/j.heliyon.2023.e16387>

Received 3 December 2022; Received in revised form 14 May 2023; Accepted 15 May 2023

Available online 17 May 2023

2405-8440/© 2023 Published by Elsevier Ltd.

This is an open access article under the CC BY-NC-ND license

(<http://creativecommons.org/licenses/by-nc-nd/4.0/>).

Table 1
Ultimate and proximate analysis of Illinois no-6 fuel.

Ultimate analysis (%)		Proximate analysis (%)	
Moisture	12	Moisture	12
Ash	16	Ash	16
Carbon	55.35	Volatile matter	33
Hydrogen	4	Fixed Carbon	39
Nitrogen	1.08		
Chlorine	0.1		
Sulfur	4		
Oxygen	7.47		
Total	100	Total	100

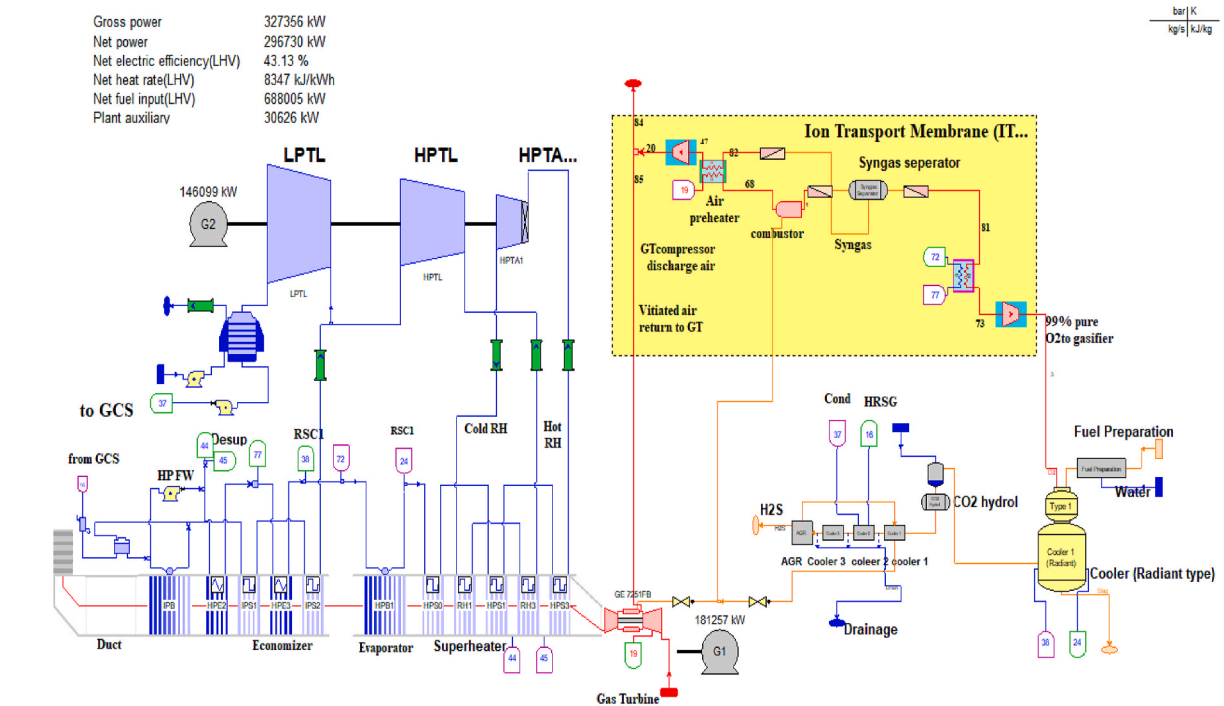


Fig. 1. Schematic Diagram of a powerplant consisting of ITM, ST, GT, GCS, Reactor.

15]. Work is underway to develop commercially viable metal-ceramic materials that are selectively permeable to oxygen ions. So-called Ion Transport Membranes are proven at research scales and are actively being commercialized. Commercial systems promise to produce hundreds to thousands of tons per day of high purity oxygen with significantly lower capital and operating expenses and with lower energy requirements [16,17].

In recent years, researchers have carried out several experiments to investigate the performance of a powerplant by integrating several energy generation and processing units such as gasifier, gas turbine, Heat Recovery Steam Generator (HRSG), Air Separation Unit (ASU) and gas clean up systems. Various researchers have reported significant improvements in power generation by increasing the yielding power, lower the emissions, lowering the cost, utilization of waste heat and water and modeling a compact power plant. The combination of the ASU with gas turbine has emerged as a key process due to high energy requirement for the ASU unit and net efficiency [18,19]. In this regard, researchers have developed the ITM, which has the potential to supply high purity O₂ to the gasifier and it can be operated with lower cost compared to the conventional ASUs.

In this study, a novel model is proposed by employing heat recovery steam generator, gas turbine, gasifier, gas clean up system, syngas separator with different subsystems such as evaporator, economizer, superheater, compressor, heat exchanger etc. Focusing on the oxygen production portion of the model, air from the gas turbine (GT) compressor is pressurized in a boost compressor and preheated in a recuperator before admission to the topping heater. Illinois no-6 is used as fuel in our proposed model which is a high volatile bituminous type of coal, and the ultimate and proximate analysis are presented in Table 1.

The air is heated to its final temperature (1088K) by burning syngas before admission to the membrane array. Oxygen ions permeate the selective membrane and form oxygen molecules on the other side. Approximately 90% of the available oxygen is separated from the air when operating around 1088K and GT compressor discharge pressures. The membrane introduces a minor

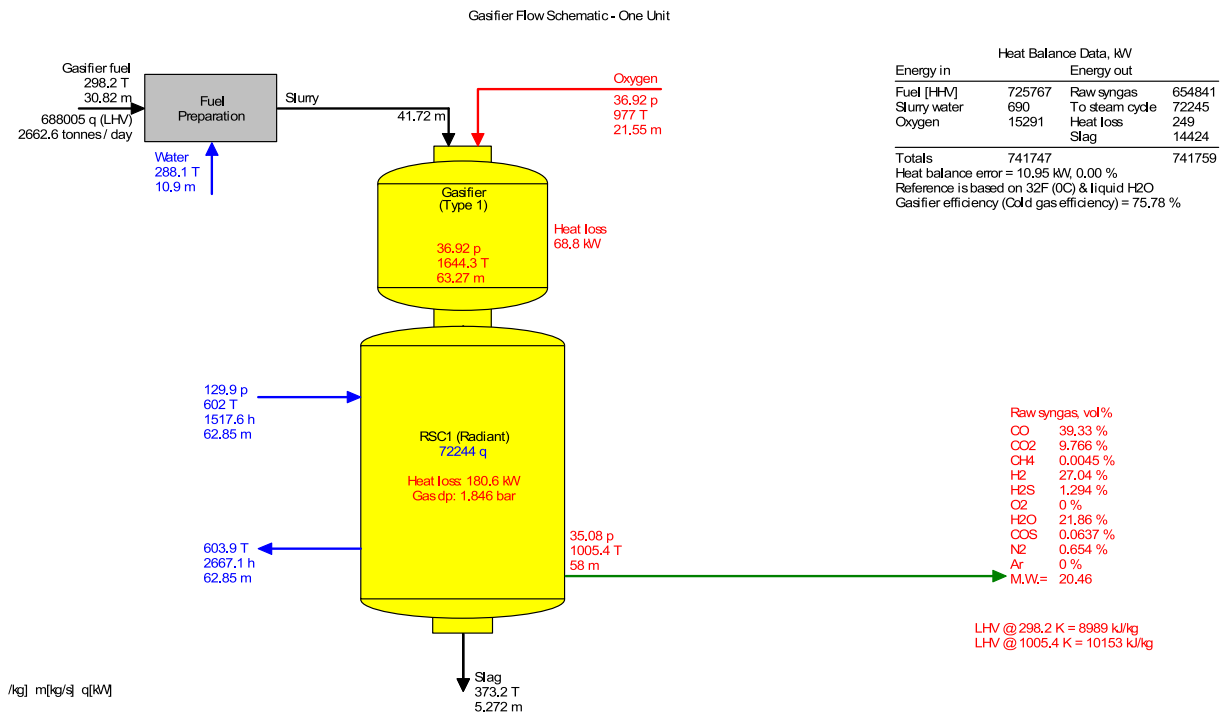


Fig. 2. Gasifier unit.

pressure loss. 99% pure oxygen exiting the array is cooled by heating feedwater and then compressed for delivery to the gasifier. Oxygen-depleted air is cooled against O₂-rich air in the recuperator and delivered to the GT for NO_x reduction and power augmentation. Pressure drops introduced by the recuperator and heat exchangers are overcome by dedicated compressors.

2. Modeling of the IGCC system with ITM

Integrated Gasification Combined Cycle is the system where the syngas produced in gasification chamber is used in a gas turbine to produce electricity [20]. It consists of a fuel preparation system, fuel source, cooler (radiant), gas clean-up system, valves, gas turbine system. Here, in this model, IGCC is combined with the ITM and the HRSG. To make the power production system more efficient these systems are combined to get the maximum efficiency for power production. In this combined system (Fig. 1), ION Transport Membrane is used for oxygen production and this oxygen is supplied in the gasifier where the oxygen mixes with water and fuel and the raw synthesis gas is produced [21]. The temperature of this raw gas is very high and for usability it is moved to the cooler (radiant) where the gas loses some amount of heat, and the temperature of the raw gases reduces. Then this raw gas goes through a gas clean-up system where the gas cools down by going through three different coolers and then hydrogen sulfide is removed from the gas. Then this clean syngas is supplied as fuel to the ITM combustor and to the GT system for combustion.

Air is also supplied to the compressor and mixes with the fuel in the GT combustor. Then the air fuel mixture goes through the turbine and hits the turbine blades for which electricity is produced due to spinning of turbine blades. Then the hot gas from the turbine enters HRSG system for the purpose of waste heat treatment and power generation. The processes which occurred in the HRSG system are discussed briefly in this paper. The hot gas is used to convert water into hot steam by passing the gas through different heating and reheating systems. In this process, the hot steam is used to establish momentum in different turbines by which electricity is produced in the generator connected with turbine shaft.

3. Synthesis gas (syngas) production in the gasifier unit

Gasifier is the chamber where synthesis gas can be produced by gasification of biomass products or other solid waste particles. Gasifier fuel contains high amount of carbon and it's the technology that produces synthesis gas by gasifying carbon containing material like biomass, coal or solid waste [22]. If gasifier fuel contains less amount of fuel, then the low-heat value will be less. So, it's better to use such fuel that contains high content of carbon. The fuel characteristics and operating conditions in the gasifier unit has great impact on the produced syngas [23,24]. There is no combustion process involved to convert carbon containing fuels into syngas.

Gasifier wall is maintained at very high temperature for gasification of solid waste or biomass. From Table 1, the amounts of different elements of fuel can be seen. The gasifier fuel after fuel preparation used in this model contains 16% ash, 12% moisture, 55.35% carbon, 4% hydrogen and other ingredients like nitrogen, sulfur and chlorine in very low amounts. The low-heat value of this

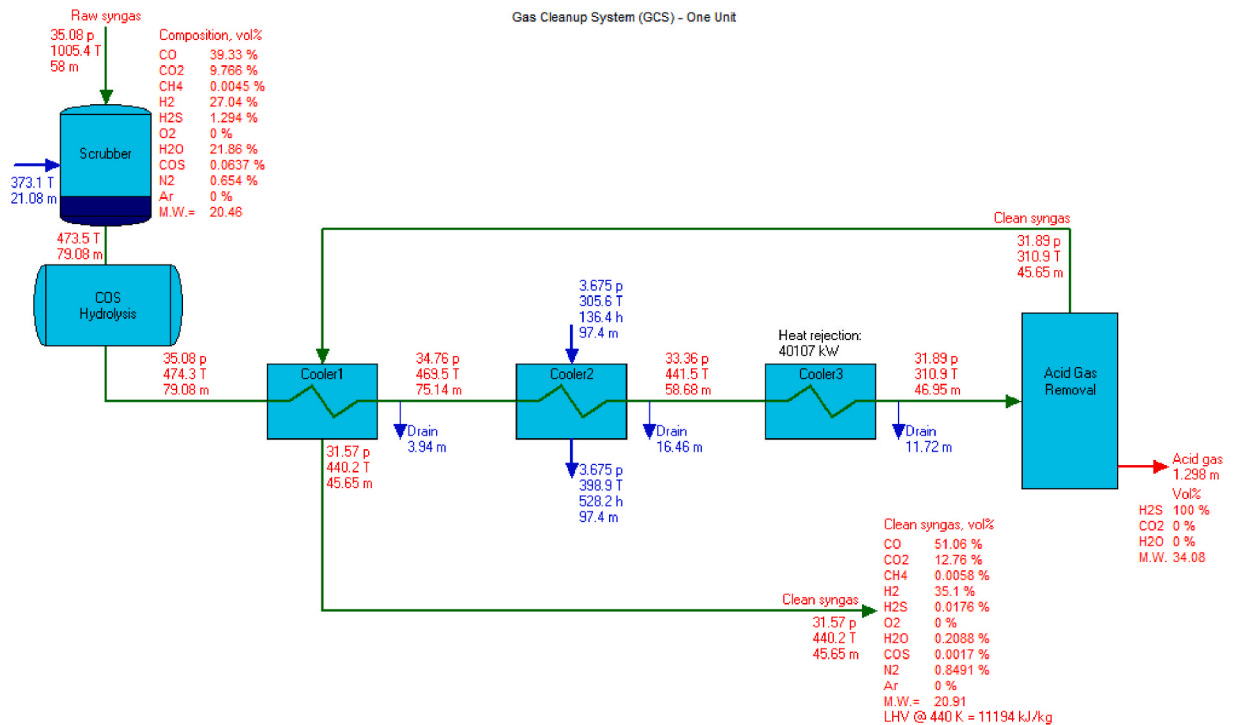


Fig. 3. Gas Clean-up system.

fuel is 22325 kJ/kg and high heat value is 23491 kJ/kg.

Before entering the gasifier (Fig. 2) the fuel is mixed with some amount of slurry water with temperature 288.1 K and pressure 3.447 bar. With the water mixed fuel pure oxygen is also supplied to the gasifier which has a temperature of 977 K and pressure 36.92 bar. The gasification is controlled at very high temperature in the gasifier and the gasifier temperature is maintained at 1644.3 K. Here, the pressure of gasifier is 36.92 bar and nominal fuel flow rate is maintained as 30.82 kg/s. After gasification different gaseous products are produced and of these products, amount of carbon dioxide, hydrogen and water is in top. Here, the efficiency of gasifier is 75.78% and heat loss in it is accounted as 68.8 kW.

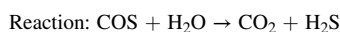
The gasifier is connected with a radiant syngas cooler with water walls where the water wall surface temperature is 678.7 K and heat loss is 180.6 kW. Water enters this cooler from economizer (HPE3) with temperature 602 K and pressure 129.89 bar. The temperature of hot syngas reduces from 1644.3 K to 1005.4 K and pressure decreases from 36.92 bar to 35.08 bar. There are three exit ways in this cooler. In one way slag is removed at mass flow rate 5.272 kg/s and temperature of slag is 373.2 K and it contains 6.479% unburnt carbon. In another way water/steam exits the cooler at 603K temperature. And in other way raw syngas exits the cooler with temperature 1005.4 K and pressure 15.08 bar. Then this raw syngas goes to gas clean-up system where this syngas is treated by different processing to make this gaseous fuel more useable.

4. Gas clean-up system

Coming out from gasifier and radiant cooler the raw syngas enters the gas clean up system (GCS) to become more useable [25]. The GCS consists of three cooler system, one AGR (acid-gas removal) system and drainage system to remove condensed water [26].

Raw syngas exiting from radiant cooler enters a scrubber which is a part of GCS (Fig. 3). Raw syngas enters here with temperature 1005.4 K and pressure 35.08 bar. One water source is added to the scrubber from which water is supplied to cool down the hot raw syngas and after processing in the scrubber temperature of raw syngas decreases to 473.5 K.

Then this raw gas goes through a CO₂ hydrolysis where hydrolysis of carbonyl sulfide (COS) is occurred, and this hydrolysis is an impurity treatment process where hydrolysis of carbonyl sulfide (COS) occurs with present of water to form hydrogen sulfide (H₂S) and carbon dioxide. Here COS is not corrosive, but H₂S is corrosive. However, COS hydrolysis should be done to get more carbon dioxide to enrich the gaseous fuel.



At the time of reaction at CO₂ hydrolysis, the syngas achieves some heat, and the temperature becomes 474.3 K.

Then this syngas enters cooler-1 and its temperature reduces from 474.3 K to 469.5 K. At 3.94 kg/s condensed water is removed from cooler-1 to a drainage system and the amount of heat removal in this cooler is 8651 kW. After this the syngas goes through cooler-2 where condensed water is pumped from water-cooled condenser which is connected to low-pressure turbine (LPTL). This inlet water

Table-2
Common solvents used in Acid-Gas Removal system.

Solvent type	Working procedure	Example of solvent
1. Chemical solvent	These are aqueous based which reacts with hydrogen sulfide reversibly after hydrolyzing in water to weak acids.	Methanolamine (MEA), methyl-diethanolamine (MDEA) [27]
2. Physical solvent	These are polar molecules having negative and positive charge which attract the polar hydrogen sulfide. Here absorption is performed at low temperature, and it also requires cooling.	Selexol, rectisol, purisol, morphysorb [28]
3. Chemical-physical/ mixed solvent	This process includes both the chemical solvents and physical solvents, and it also requires cooling.	Sulfinol, amisol [29]
4. Oxidative solvent	These solvents are used to oxidize hydrogen sulfide to elemental sulfur reacting with it where the sulfur is recovered as a solid.	Sulferox, Lo-Cat [30]

Table-3
Input and output power in different sources.

Generator power output	181257 kW
Shaft power	183830 kW
Compressor power	174901 kW
Turbine power	359875 kW
Mechanical loss	1143.2 kW
Generator loss	2573.2 kW

Sulfur dioxide is emitted at a rate of 91.1 kg/h and per year the amount of SO₂ emission is 798 metric tons. Net carbon dioxide is emitted 207316 kg/h and per year the amount of CO₂ emission is 1816088 metric tons.

with temperature 305.6 K exits cooler-2 where the exit water has a temperature 398.9 K after receiving heat from the syngas. At 16.46 kg/s condensed water is removed through the drainage system from cooler-2. After cooling in the syngas exits cooler-2 with temperature 441.5 K and the amount of heat rejection in cooler-2 is accounted as 38156 kW. Later this cooled syngas enters cooler-3 (external cooler) to become more cooled by releasing heat outside the system and the amount of heat rejection heat is accounted as 40107 kW. Here the syngas temperature decreases from 441.5 K to 310.9 K. At 11.72 kg/s condensed water is removed through the drainage from this system.

After passing external cooler syngas enters an AGR system where the syngas is treated to remove the H₂S, which can cause corrosion of materials of the operating system. Therefore, it is required to remove H₂S from syngas to use this syngas as a perfect fuel. Most known and used techniques which are used in AGR are regenerable, cyclic and solvent absorption. There are different types of solvents which are used to remove hydrogen sulfide from syngas by contacting it in an absorption tower and then the acidic gases are thermally generated in a stripping tower to remove H₂S. The most common solvents which are used in AGR system are shown in Table 2.

Using an AGR system, almost 100% of hydrogen sulfide is removed from the synthesis gas and the raw syngas is cleaned by processing in AGR. This clean syngas exits AGR with temperature 310.9 K and enters syngas reheater (cooler-1) where it gains some heat from the coming raw syngas and the exit temperature of clean syngas is 440.2 K. Carbon dioxide and hydrogen are the high amount ingredients of the clean syngas coming out from the gas clean-up system and this clean syngas exit GCS at 45.65 kg/s mass flow rate.

5. Gas turbine

Gas turbine combine cycle (GTCC) has gained much popularity in power production due to their lower emission, higher thermal efficiency, and high regulation capacity [31]. Optimizing the GTCC with the HRSG unit, higher overall efficiency can be achieved from a combine cycle power plant. Air enters in the compressor from an air source and also from the air compressor which is connected with the ITM unit. Air enters from an air source with 288.2 K temperature and 1.013 bar pressure and air from ITM air compressor enters with temperature 971.4 K and pressure 18.74 bar. At first, fuel coming out from gas clean up system enters in a valve where pressure drop occurs 1.579 bar and then divided into two ways in a splitter. In one way some amount of clean syngas enters ITM combustor and in another way the remaining part of clean syngas enters in the gas turbine system for burning to achieve high temperature. Clean syngas enters the GT system with a temperature of 440.2 K and pressure 18.74 bar. Air is discharged from the GT compressor at a temperature of 674.4 K and pressure 17.67 bar which goes through ITM air preheater. Here the efficiency of GT for low-heat-value is 38.49% and for high-heat-value it is 36.05%. Exhaust air from the turbine exits at temperature 912.6 K and pressure 1.0379 bar and then enters in the HRSG system. The turbine is connected to the generator through a shaft where mechanical power is supplied by the turbine shaft. Here some values are listed in Table 3.

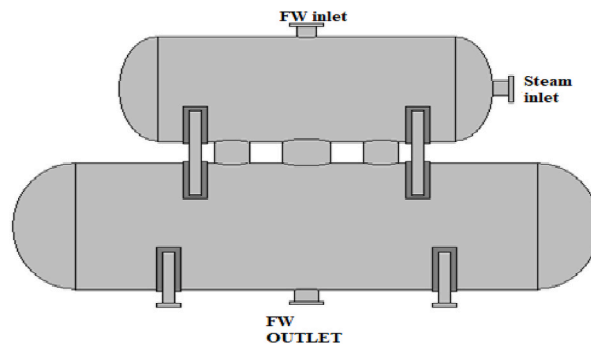


Fig. 4. Elevation view of deaerator.

6. Heat recovery steam generator

Heat recovery steam generator is a widely used technology for cogeneration where a HRSG unit contains normally economizer, evaporator, and superheater [32]. HRSG unit can utilize the waste heat from a system output that can rise the efficiency of the plant from 50% to 70–90% [33]. Usually, high temperature waste heat is much more potential than medium and lower temperature waste heat [34]. The electricity production capacity and thermal efficiency of a combine cycle power plant largely depends on the design of HRSG unit and for this reason, to utilize the exchanged heat and to improve the overall efficiency of the plant, HRSG unit must be designed carefully [35]. Water comes out from cooler-2 of Gas-Cleanup-System and enters the make-up/blowdown and after processing the make-up water exits from make-up system. This make-up water and the heating steam splitting out from evaporator (IPB) enter into the deaerator. The type of deaerator which is used in this model is horizontal heater. Here the operating pressure is 3.675 bar, operating temperature 413.7 K and total storage volume is 45773 L. The feed water exits deaerator at a mass flow rate of 100.8 kg/s, temperature 413.7 K and pressure 3675 bar.

This feedwater (FW) split into two parts in the splitter which can be seen from Fig. 4. Some amount of feed water goes through evaporator (IPB) and the other amount goes through a pump (24). In the evaporator (IPB) the enthalpy of steam increases and the exit steam from evaporator goes through a splitter from where some amount of steam goes again towards deaerator and another amount from splitter enters superheater (IPS1). In this superheater, mass flow rate of entering and exiting steam is 4.97 kg/s and temperature rises from 413 K to 533 K. This superheated steam exiting from superheater (IPS1) enters the superheater (IPS2). Here, the superheated steam gains more heat and raises its temperature from 533 K to 593 K and the mass flow rate of steam is same as before 4.97 kg/s. Then the superheated steam coming out from superheater (IPS2) goes through a pipe (22) and then mixes with the steam exiting from high pressure turbine (HPTL) in a mixer (18). Then this mixed hot steam enters low pressure turbine (LPTL).

The remaining amount of split feed water exiting from the deaerator enters a multistage centrifugal pump which is driven by an integral motor and this pump consume 2422 kW electricity. Feed water exiting from the pump enters a splitter and is divided into two ways. Some amount of feed water goes through superheater RH3 and HPS3 and the other remaining amount enters economizer HPE2. In this economizer, the inlet temperature of water is 417 K and the exit temperature is 538 K. Water exiting from economizer (HPE2) enters into a splitter where it splits into two ways. In one way some amount of water enters into a heat exchanger (53) to cool the incoming gas and in another way the remaining amount of water enters an economizer (HPE3) where the temperature of water increases from 538 to 602 K. The exiting water enters a splitter and some amount of split water enters into the cooler 1 (radiant) and the remaining amount of water mixes with the exit water from heat exchanger (53) in a mixer (54) and then the mixed water enters an evaporator (HPB1). Here in this evaporator the inlet water is converted into steam. Steam after leaving evaporator mixes with the exit steam coming from the cooler 1 (radiant) in a mixer and then this mixed steam enters a superheater (HPS0). In this superheater the inlet steam temperature is 603.9 K and the exit temperature of steam is 740.4 K. Then the superheated steam goes to another superheater (HPS1) and the steam temperature increases from 740.4 to 800.4 K. Then this superheated steam goes through superheater HPS3, and the steam temperature increases from 800.4 K to 840.4 K. Some amount of feed water is supplied before from the deaerator. This superheated steam goes through a pipe (19) and enters in the high-pressure turbine (HPTA1) and gives momentum to turbine blades to rotate. In this turbine, the overall efficiency is 87.31%, expansion power is 34016 kW, shaft power is 33912 kw and mechanical loss is 103.9 kW and the inlet and outlet temperature are 838.9 K and 633.9 K respectively. Here, high pressure end leakages are 0.2929 kg/s and 1.483 kg/s and the low-pressure leakage is 0.5784 kg/s. As expansion occurs in the turbine so both the pressure and temperature decrease and inlet and outlet pressure in this turbine are 124.1 bar and 30.97 bar respectively.

The outlet steam of turbine HPTA1 enters into a superheater (RH1) with steam temperature 631.8 K and pressure 29.81. After heating the superheated steam exits the superheater with temperature 780.3 K and pressure 28.82 bar. Here, the heat transfer rate from gas is 30370 kW and heat transfer rate to water is 30219 kW and so in this superheater heat loss is 151.2 kW. Then the superheated steam coming out from superheater RH1 enters a superheater (RH3) and after heating the temperature rises from 780.3 K to 840.3 K. Here the amount of heat loss is 60.96 kW. The superheated steam enters a high-pressure turbine (HPTL) through a pipe. As expansion occurs, the volume increases and the temperature and pressure reduce for the turbine work. In this turbine, Pressure decreases from 26.81 bar to 3.447 bar, temperature decreases from 838.7 K to 563.5 K and enthalpy also reduces. Here, the group overall efficiency for

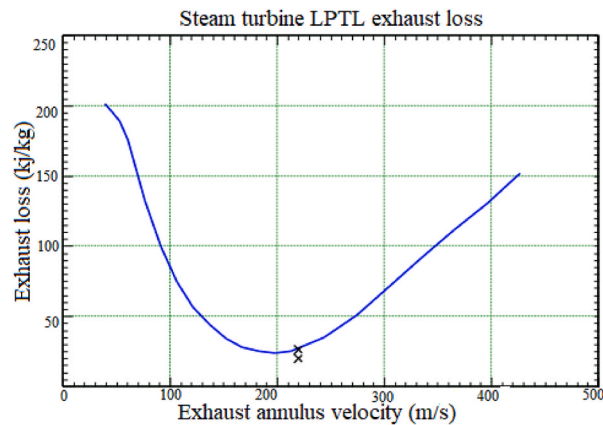


Fig. 5. Relationship between exhaust velocity and exhaust loss.

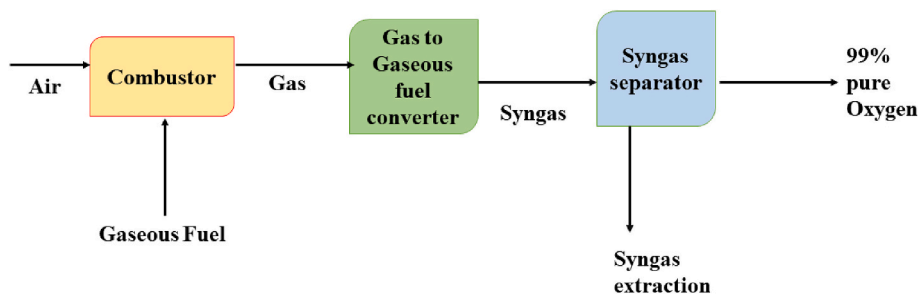


Fig. 6. Schematic diagram of Ion Transport Membrane Unit.

this turbine is 88.38%, expansion power 51031 kW, shaft power is 50875 kW and mechanical loss is 155.8 kW. High-pressure end leakage in is accounted as 1.718 kg/s. The exit steam of turbine HPTL mixes with the steam coming from superheater IPS2 in a mixer and then enters into a low-pressure turbine. In the expansion process, temperature decreases from 565 K to 303.4 K and pressure decreases from 3.447 bar to 0.0483 bar. The expansion power of this turbine is 63487 kW, shaft power is 63293 kW and the mechanical loss 193.93 kW. The overall efficiency of this turbine is 89.11% and low-pressure leakage is 0.5526 kg/s. Annulus velocity is 219.8 m/s and for this exhaust loss is accounted as 26.62 kJ/kg. Fig. 5 shows the relation between annulus velocity and exhaust loss can be realized.

With the processing of these turbines (HPTA1, HPTL, LPTL) the generator gets power to produce electricity. The generator is driven by these three turbines. The total shaft power of these three turbines equals 148080 kW which is the final shaft power goes to generator to convert mechanical power to electricity and the shaft speed is 3600 rpm. Here, the generator nameplate power is 153404 kW and nameplate efficiency 98.68%. However, the generator power output is 146099 kW and generator efficiency 98.66%. Total generator loss is accounted for 1981.5 kW which is contributed by 1738.5 kW of electrical loss and 243 kW of mechanical loss.

The exit steam from low-pressure turbine (LPTL) enters in a water-cooled condenser and some amount of cooling water is pumped in this condenser from a water source. The pump type is vertical turbine driven by an integral motor and its mechanical and isentropic efficiency is 97% and 87%, respectively. After cooling and condensation some amount of water is carried out through a pipe in a water sink and the remaining amount of water is pumped to cooler 2 of gas clean-up system.

7. Ion transport membrane (ITM) unit

Ion Transport Membrane is a recently developed technology to produce pure oxygen from syngas [36]. ITM technology emerges as a potential alternative of cryogenic air separation system due to the permeability of oxygen at much higher temperature (700–1000 °C) with high purity and lower expense [37]. In their studies, they were mainly focused on chemical reactions that occurred inside the ITM reactor. An ITM unit can also be employed as catalytic partial oxidation reactor to produce synthesis gas [38]. There are different companies in developed countries which are working to develop ceramic membranes for the purpose of oxygen separation from hot air. Researchers have carried out several experiments to enhance the oxygen permeability, durability, stability and inner phenomena to prepare ITM technology for commercialization [39–41]. Different air products and various chemicals are used to develop an ion transport membrane system. The ion transport membrane system is based on ceramic membranes which operate at very high temperature to produce oxygen. These membranes carry out the separation of oxygen from air of very high temperatures like 900–1100 K. There is no requirement of any electrodes or any electrical circuit to operate in the ion transport membrane system.

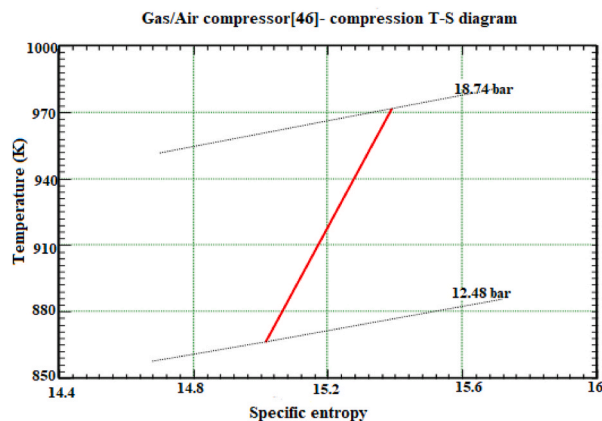


Fig. 7. T-S diagram for Gas/Air compressor (46).

Table 4

Amount of gas emissions from different components of the power plant.

Emitted gas	Plant component	Amount (kg/hr)	Total (kg/hr)	Tonne/year
SO ₂	Combustor	5.927	97.027	660.4
	Gas turbine	91.1		
CO ₂	Combustor	13488	220804	1600836
	Gas turbine	207316		

Table 5

Summary of the proposed powerplant.

Summary	Unit	Amount
Annual exported electricity	kWh	2151 × 10 ⁶
Annual fuel imported	Tj	17957
Annual CO ₂ emission	ktonne	1601
Annual water imported	l	12.1 × 10 ⁶
Annual captured CO ₂	ktonne	0
Net electric efficiency of plant	%	43.13
Gross power	kW	327356
Net Power	kW	296730
Gross electric efficiency (LHV)	%	47.58

The O₂ diffuses from the high oxygen partial pressure side towards the low oxygen partial pressure side, maintaining overall charge neutrality via counterbalancing electron flux. The air is heated to its final temperature (1088K) by burning syngas before admission to the membrane array. Oxygen ions permeate the selective membrane and form oxygen molecules on the other side. Approximately 90% of the available oxygen is separated from the air when operating around 1088K and GT compressor discharge pressures.

In the combustor, air is burnt at very high temperature (900–1100 K) and clean syngas is used as fuel to burn the air (Fig. 6). Air from gas turbine compressor enters into an air compressor with temperature 674.5 K and pressure 17.67 bar. The exit temperature and pressure from this air compressor are 869.5 K and 15.369 bar. This hot air then goes to a combustor to become more heated by burning gaseous fuel which exits from gas clean up system and then coming through valve and splitter. This gaseous fuel enters the combustor with a temperature of 440.2 K and pressure 16.91 bar.

After burning in the combustor, the air achieves a temperature of 1088.7 K. Combustion is controlled by the specified outlet temperature. Fuel inlet at low heat value is 30641 kW, at high heat value 32715 kW and combustor heat loss is 92.66 kW. Then the hot gas enters in a converter and here the hot gas is converted into gaseous fuel and then goes to the syngas separator. In this separator, syngas is separated into two portions. In one exit way, oxygen-rich gas is exited where the amount of oxygen is 99%, nitrogen 0.9943% and sulfur dioxide 0.0038%. In another way the syngas is extracted from the syngas separator where the amount of nitrogen is 91.33%, carbon dioxide 2.649%, oxygen 2.278% and argon 1.102%. This extraction syngas is in gaseous fuel form with much high temperature and this gaseous fuel is converted into air in a converter. Then this hot air (1088.7 K) enters an air preheater, and its temperature reduces to 866.5 K by releasing heat to the incoming air coming from GT compressor. Then this gas with temperature 866.5 K goes through a gas/air compressor where its temperature increases to 971.4 K and pressure increases from 12.47 bar to 18.74 bar. Here the compression power is 11287 kW, shaft power 11309 kW, mechanical loss 22.62 kW, and mechanical efficiency of this compressor is 99.8%.

From Fig. 7, the T-S diagram shows the change of properties of air. Then the compressed gas goes through a splitter where it divides in two ways. In one way some amount of gas is rejected in a gas sink and remaining amount of gas enters gas turbine compressor with temperature 971.4 K and pressure 18.74 bar.

8. Results and discussion

The amount of gas emission can be found in Table 4 from where it can be seen that approximately 1601 ktonne of CO₂ and 660.4 ktonne of SO₂ are emitted from the plant. As no carbon capture technology was integrated with this system, the emitted gas dissipated through the stack.

Table 5 represents the output summary of the proposed plant from where it can be seen that 47.58% of gross efficiency can be achieved from this proposed model which comparatively higher than the model developed by Shi et al. [42] where they employed cryogenic ASU with IGCC based powerplant and obtained 40.25% net efficiency. However, no carbon capture technology was applied to capture the massive amount of CO₂ from the plant and further development is possible by integrating a potential CCS technology with this model.

9. Conclusions

Power consumption rate is reduced for the auxiliary components which is possible due to larger amount of air extraction rate. The air compressor consumes less amount of power which causes an increase in net efficiency of system and this increase in net efficiency is very low because of the loss of air mass flow rate from GT combustor. In comparison with the cryogenic air separator, the ITM system has capacity to increase net power production and improve net efficiency by reducing auxiliary load with a small incremental fuel demand. However, some additional fuel is burnt to heat the air for the ITM, so the fuel consumption increases. Nonetheless, the net electric efficiency improves from about 40.25% in the base (cryogenic ASU) case to about 47.58% in this case, a noteworthy increase as well as annual gross power was obtained as 327356 kW. A novel design of ITM integrated powerplant is proposed in this paper that can give direction for further development of a powerplant and to implement for commercialization. Integrating a potential CO₂ capture technology can further improve the efficiency and potentiality of the powerplant.

Author contribution statement

Arnob Das: Conceived and designed the analysis; Analyzed and interpreted the data; Wrote the paper.

Susmita Datta Peu: Contributed analysis tools or data; Wrote the paper.

Md. Sanowar Hossain: Analyzed and interpreted the data; Wrote the paper.

Barun Kumar Das: Conceived and designed the analysis; Contributed analysis tools or data.

Data availability statement

Data included in article/supplementary material/referenced in article.

Declaration of competing interest

The authors declare that they have no known competing financial interests or personal relationships that could have appeared to influence the work reported in this paper.

References

- [1] A. Das, S.D. Peu, A comprehensive review on recent advancements in thermochemical processes for clean hydrogen production to decarbonize the energy sector, *Sustainability* 14 (2022), 11206, <https://doi.org/10.3390/SU141811206>.
- [2] E. Zafeiriou, N. Sariannidis, S. Tsiantikoudis, A. Das, S. Datta Peu, M. Abdul Mannan Akanda, et al., Peer-to-Peer energy trading pricing mechanisms: towards a comprehensive analysis of energy and network service pricing (NSP) mechanisms to get sustainable enviro-economical energy sector, *Energies* 16 (2023), 2198, <https://doi.org/10.3390/EN16052198>.
- [3] P. Mahapatra, B.W. Bequette, Design and control of an elevated-pressure air separations unit for IGCC power plants in a process simulator environment, *Ind. Eng. Chem. Res.* 52 (2012) 3178–3191, <https://doi.org/10.1021/IE301034E>.
- [4] H. Liu, W. Ni, Z. Li, L. Ma, Strategic thinking on IGCC development in China, *Energy Pol.* 36 (2008) 1–11, <https://doi.org/10.1016/J.ENPOL.2007.08.034>.
- [5] C. Descamps, C. Bouallou, M. Kanniche, Efficiency of an integrated gasification combined cycle (IGCC) power plant including CO₂ removal, *Energy* 33 (2008) 874–881, <https://doi.org/10.1016/J.ENERGY.2007.07.013>.
- [6] J. Zhang, Z. Zhou, L. Ma, Z. Li, W. Ni, Efficiency of wet feed IGCC (integrated gasification combined cycle) systems with coal–water slurry preheating vaporization technology, *Energy* 51 (2013) 137–145, <https://doi.org/10.1016/J.ENERGY.2012.12.024>.
- [7] L. Han, G. Deng, Z. Li, Y. Fan, H. Zhang, Q. Wang, et al., Simulation and optimization of ion transfer membrane air separation unit in an IGCC power plant, *Appl. Therm. Eng.* 129 (2018) 1478–1487, <https://doi.org/10.1016/J.APPLTHERMALENG.2017.10.131>.
- [8] K. Ståhl, M. Neergaard, IGCC power plant for biomass utilisation, Värnamo, Sweden, *Biomass Bioenergy* 15 (1998) 205–211, [https://doi.org/10.1016/S0961-9534\(98\)00025-7](https://doi.org/10.1016/S0961-9534(98)00025-7).
- [9] J.S. Rhodes, D.W. Keith, Engineering economic analysis of biomass IGCC with carbon capture and storage, *Biomass Bioenergy* 29 (2005) 440–450, <https://doi.org/10.1016/J.BIOMBIOE.2005.06.007>.
- [10] H.M. Sheikh, A. Ullah, K. Hong, M. Zaman, Thermo-economic analysis of integrated gasification combined cycle (IGCC) power plant with carbon capture, *Chem. Eng. Process. Proc. Inten.* 128 (2018) 53–62, <https://doi.org/10.1016/J.CEP.2018.04.007>.

- [11] J. Parraga, K.R. Khalilpour, A. Vassallo, Polygeneration with biomass-integrated gasification combined cycle process: review and prospective, *Renew. Sustain. Energy Rev.* 92 (2018) 219–234, <https://doi.org/10.1016/J.RSER.2018.04.055>.
- [12] T. Chmielniak, M. Sciazko, Co-gasification of biomass and coal for methanol synthesis, *Appl. Energy* 74 (2003) 393–403, [https://doi.org/10.1016/S0306-2619\(02\)00184-8](https://doi.org/10.1016/S0306-2619(02)00184-8).
- [13] B.v. Piguave, S.D. Salas, D. de Cecchis, J.A. Romagnoli, Modular framework for simulation-based multi-objective optimization of a cryogenic air separation unit, *ACS Omega* 7 (2022) 11696–11709, <https://doi.org/10.1021/acsomega.1c06669>.
- [14] R. Ortega-Lugo, J.A. Fabián-Anguiano, O. Ovalle-Encinia, C. Gómez-Yáñez, B.H. Zeifert, J. Ortiz-Landeros, Mixed-conducting ceramic-carbonate membranes exhibiting high CO₂/O₂ permeation flux and stability at high temperatures, *J. Adv. Ceram.* 9 (2020) 94–106, <https://doi.org/10.1007/S40145-019-0352-2/METRICS>.
- [15] V.v. Belousov, S.v. Fedorov, An oxygen-permeable bilayer MIEC-redox membrane concept, *ACS Appl. Mater. Interfaces* 10 (2018) 21794–21798, https://doi.org/10.1021/ACSAMI.8B05315/SUPPL_FILE/AM8B05315_SI_001.PDF.
- [16] D. Zhang, X. Zhang, Y. Jiang, S. Ye, L. Qiang, B. Lin, A stable Zr-Y co-doped perovskite BaCo_{0.4}Fe_{0.4}Zr_{0.1}Y_{0.1}O_{3-δ} ceramic membrane for highly efficient oxygen separation, *Sep. Purif. Technol.* 295 (2022), 121206, <https://doi.org/10.1016/J.SEPPUR.2022.121206>.
- [17] Z. Zhang, W. Zhou, Y. Chen, D. Chen, J. Chen, S. Liu, et al., Novel approach for developing dual-phase ceramic membranes for oxygen separation through beneficial phase reaction, *ACS Appl. Mater. Interfaces* 7 (2015) 22918–22926, https://doi.org/10.1021/ACSAMI.5B05812/SUPPL_FILE/AM5B05812_SI_001.PDF.
- [18] A.R. Smith, J. Klosek, A review of air separation technologies and their integration with energy conversion processes, *Fuel Process. Technol.* 70 (2001) 115–134, [https://doi.org/10.1016/S0378-3820\(01\)00131-X](https://doi.org/10.1016/S0378-3820(01)00131-X).
- [19] H.C. Frey, Y. Zhu, Improved system integration for integrated gasification combined cycle (IGCC) systems, *Environ. Sci. Technol.* 40 (2006) 1693–1699, <https://doi.org/10.1021/es0515598>.
- [20] C. Descamps, C. Bouallou, M. Kanniche, Efficiency of an integrated gasification combined cycle (IGCC) power plant including CO₂ removal, *Energy* 33 (2008) 874–881, <https://doi.org/10.1016/J.ENERGY.2007.07.013>.
- [21] P.N. Dyer, R.E. Richards, S.L. Russek, D.M. Taylor, Ion transport membrane technology for oxygen separation and syngas production, *Solid State Ionics* 134 (2000) 21–33, [https://doi.org/10.1016/S0167-2738\(00\)00710-4](https://doi.org/10.1016/S0167-2738(00)00710-4).
- [22] A. Sitka, W. Jodkowski, P. Szulc, D. Smykowski, B. Szumilo, Study of the properties and particulate matter content of the gas from the innovative pilot-scale gasification installation with integrated ceramic filter, *Energies* 14 (2021) 7476, <https://doi.org/10.3390/EN14227476>.
- [23] R. Tavares, E. Monteiro, F. Tabet, A. Rouboa, Numerical investigation of optimum operating conditions for syngas and hydrogen production from biomass gasification using Aspen Plus, *Renew. Energy* 146 (2020) 1309–1314, <https://doi.org/10.1016/J.RENENE.2019.07.051>.
- [24] J. Li, K. Xu, X. Yao, S. Chen, Prediction and optimization of syngas production from steam gasification: numerical study of operating conditions and biomass composition, *Energy Convers. Manag.* 236 (2021), 114077, <https://doi.org/10.1016/J.ENCONMAN.2021.114077>.
- [25] A. Giuffrida, M.C. Romano, G. Lozza, Efficiency enhancement in IGCC power plants with air-blown gasification and hot gas clean-up, *Energy* 53 (2013) 221–229, <https://doi.org/10.1016/J.ENERGY.2013.02.007>.
- [26] E.I. Koystoumpa, K. Atsonios, K.D. Panopoulos, S. Karellas, E. Kakaras, J. Karl, Modelling and assessment of acid gas removal processes in coal-derived SNG production, *Appl. Therm. Eng.* 74 (2015) 128–135, <https://doi.org/10.1016/J.APPLTHERMALENG.2014.02.026>.
- [27] A. Akachuku, P.A. Osei, B. Decardi-Nelson, W. Srisang, F. Pouryousefi, H. Ibrahim, et al., Experimental and kinetic study of the catalytic desorption of CO₂ from CO₂-loaded monoethanolamine (MEA) and blended monoethanolamine – methyl-diethanolamine (MEA-MDEA) solutions, *Energy* 179 (2019) 475–489, <https://doi.org/10.1016/J.ENERGY.2019.04.174>.
- [28] W.H. Chen, S.M. Chen, C.I. Hung, Carbon dioxide capture by single droplet using Selexol, Rectisol and water as absorbents: a theoretical approach, *Appl. Energy* 111 (2013) 731–741, <https://doi.org/10.1016/J.APENERGY.2013.05.051>.
- [29] A. Wilk, L. Wicław-Solny, A. Tatarczuk, A. Krótki, T. Spietz, T. Chwoła, Solvent selection for CO₂ capture from gases with high carbon dioxide concentration, *Kor. J. Chem. Eng.* 34 (2017), <https://doi.org/10.1007/S11814-017-0118-X>, 8 2017;34:2275–2283.
- [30] D.A. Dalrymple, T.W. Trofe, J.M. Evans, Liquid redox sulfur recovery options, costs, and environmental considerations, *Environ. Prog.* 8 (1989) 217–222, <https://doi.org/10.1002/EP.3300080412>.
- [31] Z. Zhong, Z. Huo, X. Wang, F. Liu, Y. Pan, New steam turbine operational mode for a gas turbine combine cycle bottoming cycle system, *Appl. Therm. Eng.* 198 (2021), 117451, <https://doi.org/10.1016/j.applthermaleng.2021.117451>.
- [32] Y. Farahani, A. Jafarian, O. Mahdavi Keshavar, Dynamic simulation of a hybrid once-through and natural circulation heat recovery steam generator (HRSG), *Energy* 242 (2022), 122996, <https://doi.org/10.1016/j.energy.2021.122996>.
- [33] H.I. Onowiona, V.I. Ugursal, Residential cogeneration systems: review of the current technology, *Renew. Sustain. Energy Rev.* 10 (2006) 389–431, <https://doi.org/10.1016/j.rser.2004.07.005>.
- [34] A. Ahmed, K.K. Esmail, M.A. Irfan, F.A. Al-Mufadi, Design methodology of heat recovery steam generator in electric utility for waste heat recovery, *Int. J. Low Carbon Technol.* 13 (2018) 369–379, <https://doi.org/10.1093/ijlct/cty045>.
- [35] J.I. Manassaldi, S.F. Mussati, N.J. Scenna, Optimal synthesis and design of heat recovery steam generation (HRSG) via mathematical programming, *Energy* 36 (2011) 475–485, <https://doi.org/10.1016/j.energy.2010.10.017>.
- [36] M.A. Habib, H.M. Badr, S.F. Ahmed, R. Ben-Mansour, K. Mezghani, S. Imashuku, et al., A review of recent developments in carbon capture utilizing oxy-fuel combustion in conventional and ion transport membrane systems, *Int. J. Energy Res.* 35 (2011) 741–764, <https://doi.org/10.1002/ER.1798>.
- [37] D. Shin, S. Kang, A spatially resolved physical model of an ion transport membrane reactor for system development, *J. Membr. Sci.* 586 (2019) 292–305, <https://doi.org/10.1016/j.memsci.2019.05.080>.
- [38] P.N. Dyer, R.E. Richards, S.L. Russek, D.M. Taylor, Ion transport membrane technology for oxygen separation and syngas production, *Solid State Ionics* 134 (2000) 21–33, [https://doi.org/10.1016/S0167-2738\(00\)00710-4](https://doi.org/10.1016/S0167-2738(00)00710-4).
- [39] Y. Huang, C. Zhang, X. Wang, D. Li, L. Zeng, Y. He, et al., High CO₂ resistance of indium-doped cobalt-free 60 wt.%Ce_{0.9}Pr_{0.1}O_{2-δ}-40 wt.%Pr_{0.6}Sr_{0.4}Fe_{1-x}In_xO_{3-δ} oxygen transport membranes, *Ceram. Int.* 48 (2022) 415–426, <https://doi.org/10.1016/j.ceramint.2021.09.117>.
- [40] Y. Liu, H. Cheng, Q. Sun, X. Xu, S. Chen, Q. Xu, et al., Phase transition and oxygen permeability of Pr_{0.6}Sr_{0.4}FeO_{3-δ} ceramic membrane at high temperature, *J. Eur. Ceram. Soc.* 41 (2021) 1975–2083, <https://doi.org/10.1016/j.jeurceramsoc.2020.10.064>.
- [41] D. Li, X. Wang, W. Tan, Y. Huang, L. Zeng, Y. He, et al., Influences of Al substitution on the oxygen permeability through 60 wt.%Ce_{0.9}La_{0.1}O_{2-δ}-40 wt.%La_{0.6}Sr_{0.4}Co_{1-x}Al_xO_{3-δ} composite membranes, *Sep. Purif. Technol.* 274 (2021), 119042, <https://doi.org/10.1016/j.seppur.2021.119042>.
- [42] B. Shi, W. Xu, E. Wu, W. Wu, P.C. Kuo, Novel design of integrated gasification combined cycle (IGCC) power plants with CO₂ capture, *J. Clean. Prod.* 195 (2018) 176–186, <https://doi.org/10.1016/J.JCLEPRO.2018.05.152>.